



HAL
open science

Using solar air heating for fruit drying: thermo-economic and environmental studies

Rabih Murr, Georges El Achkar, Jalal Faraj, Hicham El Hage, Cathy
Castelain, Mahmoud Khaled

► To cite this version:

Rabih Murr, Georges El Achkar, Jalal Faraj, Hicham El Hage, Cathy Castelain, et al.. Using solar air heating for fruit drying: thermo-economic and environmental studies. *International Journal of Thermofluids*, 2023, 18, pp.100366. 10.1016/j.ijft.2023.100366 . hal-04104409

HAL Id: hal-04104409

<https://hal.science/hal-04104409>

Submitted on 24 May 2023

HAL is a multi-disciplinary open access archive for the deposit and dissemination of scientific research documents, whether they are published or not. The documents may come from teaching and research institutions in France or abroad, or from public or private research centers.

L'archive ouverte pluridisciplinaire **HAL**, est destinée au dépôt et à la diffusion de documents scientifiques de niveau recherche, publiés ou non, émanant des établissements d'enseignement et de recherche français ou étrangers, des laboratoires publics ou privés.

Using solar air heating for fruit drying: Thermo-economic and environmental studies

Rabih Murr¹, Georges El Achkar¹, Jalal Faraj^{1,2}, Hicham El Hage¹, Cathy Castelain³, and Mahmoud Khaled^{1,4,*}

¹*Energy and Thermo-Fluid group – Lebanese International University LIU – Bekaa – Lebanon*

²*Energy and Thermo-Fluid group – The International University of Beirut BIU – Beirut – Lebanon*

³*Laboratory of Thermal Energy of Nantes, LTEN, Polytech' Nantes, University of Nantes, Nantes-France*

⁴*Center for Sustainable Energy & Economic Development (SEED), Gulf University for Science & Technology, Kuwait*

**Corresponding author: mahmoud.khaled@liu.edu.lb*

Abstract

Air heating is currently an essential part in many industrial and residential applications. One of its disadvantages is the higher energy consumption. Therefore, the renewable energy sources present now different solutions in order to decrease the energy consumption and to enhance the performance of existing systems by the hybridization. For these reasons the energy management at all levels became one of the most important research. In this context, the present paper proposes a design for a solar air heater that could be applied in more than one application. A modeling and an experimental study are presented. The presented solar air heating system allows reducing the energy consumption by replacing completely or partially an electrical air heating system. In addition, an in-house code is developed in order to simulate the suggested solar air heater and to study its performance. The experimental setup is implemented and designed to validate the developed code. Accordingly, a relative error of the modeling is estimated and it varies between 4 and 14%. Finally, the system is evaluated economically and environmentally by assessing the effect of replacing the electrical heating system of a fruit dryer by the suggested solar heating. It has been shown that adopting such system allows to save up to \$106 per year and to reduce about 2045 kg of carbon dioxide emission.

1. Introduction

Energy is the backbone of the daily operation in plenty of applications and represents nowadays the focus of millions of researchers in different areas like automotive [1-3] where the heat transfer process has a major impact on the cooling systems performance and energy consumption, space heating [4], fruit drying [5-6], clothes drying [7] and electric energy production [8]. The actual world tendency in energy researches is toward energy consumption and carbon dioxide emission reduction [9-11]. This can be mainly accomplished by renewable energy and energy management [12-13] in the objective of energy saving and systems thermal efficiency improvement [14].

Currently, the solar energy became more and more essential source of energy for thermal cooling and heating applications [15] and/or to provide electrical power using the photovoltaic panels at all levels: industrial, agriculture and residential applications [16-20]. Thermal solar panels are mainly used for heating water or for heating air. For this reason, the Solar Air Heater (SAH) became key tool in some industrial applications where it could play an important role to save money and reduce environmental impact [21-22]. The SAH is a simple and efficient thermal device. It consists of an absorber plate or solar collector that convert the solar energy to heat one. The sun irradiation heat flux is absorbed by the solar collector and then converted to heat a circulating air [23]. There are different types of solar air heaters: flat plate collector, evacuated tube collector and compound parabolic collectors. Flat plate collectors are one of the most used collectors in solar systems and are used for low-Temperature applications where the demanded temperatures is between 30 and 100°C. The main components of flat plate collectors are a dark colored flat plate absorber (usually made of copper, aluminum or steel) with an insulated cover accompanied by a selective layer to increase the solar radiation absorption and an insulated backing. Evacuated tube collectors have been suggested as functional solar thermal energy collectors since the early twentieth century. They work on the rule of using vacuum as an excellent insulator fence, preventing heat loss between the absorber plate and the atmospheric primarily due to convection and conduction [24]. Compound parabolic collectors have the ability of reflecting all the incident radiation in wide limits range to the receiver. The need of moving the concentrator to tracking the sun can be neglected by using a trough with two sections of a parabola facing each other. They can be used for high temperatures applications, from 60°C to 240°C [25]. The thermal performance of the SAH depend on several parameters which are the geometrical parameters and the thermal parameters that are based on the conservation of mass and energy. For this reason, the design of SAH should deal with the thermal behavior. The enhancement and the optimum design is discussed by Adel Hegazy [26]. The main objective was to find an optimum channel geometry for a conventional SAH design but for a constant flow operation, where the flow rate is one of the most important variables that should be taken into consideration for an optimum design. An investigation for efficient design of counter flow double pass curved SAH was suggested by Kumar et al. [27]. The interesting numerical investigation focused on introducing arched baffles where the design is considered for various geometric parameters (pitch, angle of attack) in order to enhance the thermal performance by making an analysis of effectiveness. Accordingly, the relative maximum enhancement is estimated in the range of 20-28% but this study should be accomplished by an experimental investigation. In order to enhance also the performance of SAH, Chand et al [28] suggested using louvered fins collector for SAH where the obtained results are compared with a plane SAH. Accordingly, the thermal efficiency is increased by using fins. It was shown that the thermal efficiency of louvered fin spacing 2 cm and 5 cm is higher as compared to plane solar air heater which is 106.7% and 59.45% respectively. Arkar et al [29] performed a design and modelling of a SAH. The system is composed of latent heat storage system and air vacuum tubes. The performance of the system was analyzed by experimental validation of a numerical model of the system. The results of the analysis revealed that the solar heating fraction of 63% can be attained. Recently, Saxena et al [30] presented a thermodynamic review on solar air heaters including their developments since 1877. The developed techniques have been adopted to enhance the thermal performance of solar air heaters and maximize the benefits from using solar air heaters. The review performed by Srivastava and Rai [31] on solar air heaters facilitated discussions and evaluations of the techniques and findings obtained by researchers. An experimental and numerical investigation is presented in [32] that demonstrates an increase of the thermal performance Triangular Solar air heater roughened absorber surface. The experimental

results indicate an average 4.93% thermal efficiency increase and 4.41% of exergy. Lamrani et al [33] showed in their study the feasibility of solar air heater coupled with a heat recovery unit, applied to conventional wood dryers. Their numerical analysis is extended to study the effect of the suggested system on economic benefits during hot and cold climates. Annual energy consumption reduction up to 41% was noticed. It is also shown that using a combined heat recovery unit and PVT collector improved significantly the energy efficiency of conventional dryers and reduced by about 67.5% and 49.5% the yearly energy consumption in hot and cold climates, respectively. According to the brief literature review, it was pleasantly noted that the solar air heater could be used in wide range of applications and it could enhance the thermal performance/efficiency of existing system. For these reasons, in the present study, a thermal, economic and environmental modelling of a solar air heater is developed and an experimental study was executed to validate the model results. The aim of this work is to determine the outlet air temperature for a given length of the solar air heater tubes so that this temperature is suitable for drying many kinds of food at low temperatures around 50-80°C, like: fruits, vegetables, sea food, spices and cereals.

The originality of the present paper resides in the following points:

1. It proposes a new eco-friendly system that can be used as dryer for fruits or other substances like clothing.
2. An in-house code of a solar air heater has been developed based on a thermal modelling validated experimentally.
3. A parametric study can be performed easily with minimum computational time and cost.
4. It offers useful system and model for solar thermal systems.

The rest of this paper is organized as follows. Section 2 describes the design of the solar air heater. Section 3 presents the modelling integrated in the in-house code which is detailed in section 4. In section 5, the experimental study is presented in order to validate this model. Sections 6 and 7 are devoted to reveal the results for a case study on fruit drying and finally, section 8 presents the conclusions of this paper.

Nomenclature

A	area (m ²)
C _p	specific heat of air (kJ/kg.K)
d	diameter (m)
E	energy (kWh)
f	surface fraction
G	irradiance (W/m ²)
h	convective heat transfer coefficient (W/m ² .K)
K	thermal conductivity of tube (W/m.K)
L	length of the tube (m)
M	mass (kg)
<i>m</i>	mass flow rate (kg/s)
N	number of batches

Nu	Nusselt number
P	Percentage
Pr	Prandtl number of air (0.705 at temperature 30°C)
r	radius (m)
R	resistance (K/W)
R	gas constant of air (287 J/kg.K)
Re	Reynolds number
Ro	density of air (kg/m ³)
SAH	Solar Air Heater
SM	saved money (\$)
T	temperature, °C
t	time (s)
ΔT	temperature difference (°C)
μ	dynamic viscosity of air (1.91×10 ⁻⁵ kg/m.s)
ρ	reflectivity
α	absorptivity
ε	emissivity
τ	transmissivity
σ	Stefan-Boltzmann constant (5.67×10 ⁻⁸ W. m. K ⁻⁴)

Subscripts

cond,t	conduction in the tube
conv,a	convection of air
a	air
avg	average
c	cross section
d	drying
e	effective
i	inner
l	lateral
o	outer
s	surface
s	solar
tot	total
t	tube

2. Solar air heater design

In this study, a solar air heater is designed to heat up an air flow to 50-80°C and then to be used in order to dry food. The solar air heater consists of air tubes having high thermal conductivity like iron painted black color to optimize the absorption of solar rays since for black bodies the absorptivity and emissivity are approximately equal and close to 1. Ambient air enters the solar air

heater tubes from the bottom where it is heated by the solar rays hitting the solar air heater. Then, hot air exits the solar air heater from the top. These tubes are covered by a double glazing to reduce the thermal losses to the surroundings by conduction and convection. The whole system is inclined by a certain angle with the horizontal depending on the latitude and longitude of the region where the system is placed. Figure 1-a illustrates a 3D drawing of the designed solar air heater: the air inlet and outlet are shown on the left side, the tubes are placed in snake shape in order to reduce the area of the solar air heater and the upper side of these tubes are covered by a double glazing layer that permits to the solar radiation to be transmitted to the tubes and reduce the thermal losses (mainly convection) from the tubes to the surroundings at the same time.

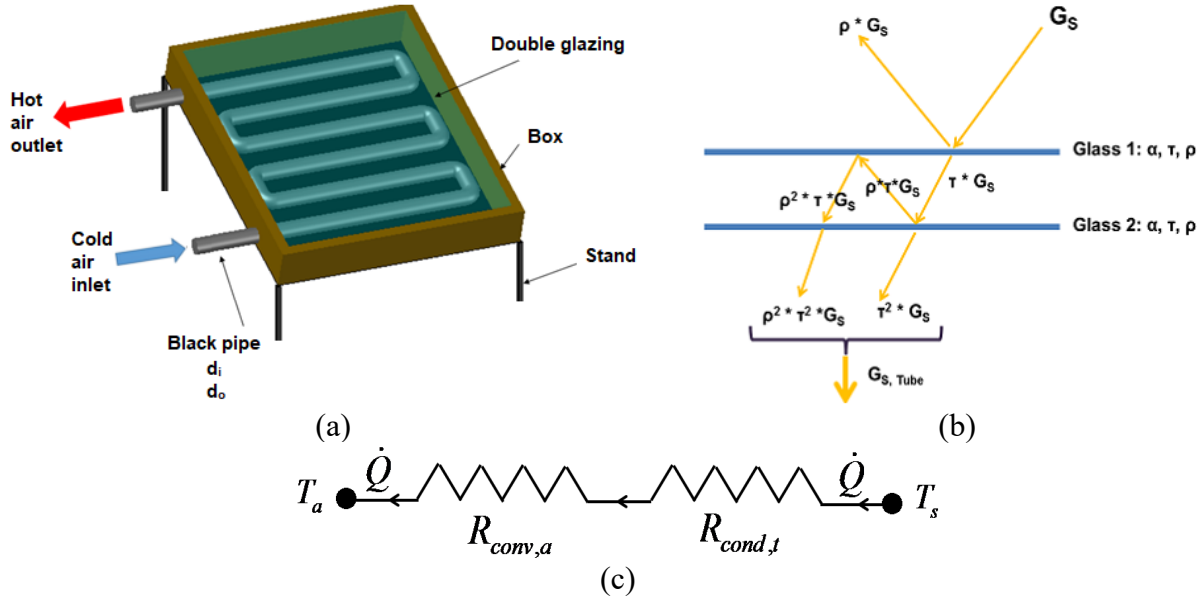


Fig. 1. (a) Solar air heater design, (b) Schematic of the radiation heat transfer through the two glass layers and (c) Thermal resistances between T_s and T_a

3. Thermal modelling

To design a solar air heater to be used to heat an air flow to a certain temperature, a thermal modelling is performed and is detailed in this section. This model relies on the mass and energy principles with steady state conditions.

The rate of heat gains by the air passing through the system is calculated as follows.

$$\dot{Q} = \dot{m} \cdot C_p \cdot \Delta T_1 \quad (1)$$

Where “ \dot{m} ” is the air flow rate, “ C_p ” is the air specific heat at constant pressure and “ ΔT_1 ” is the difference of temperature between inlet and outlet air ($T_o - T_i$).

Since the air tubes are covered by a double glazing, the solar irradiance “ G_s ”, which is measured with a Pyranometer, is not equal to the radiation absorbed by the tubes. The two glass layers are similar (same absorptivity “ α ”, transmissivity “ τ ”, reflectivity “ ρ ” and emissivity “ ϵ ”) and

separated by a distance “e”. The transmitted radiation to the tubes “ $G_{s,tube}$ ” is calculated as function of the solar irradiance received from the sun “ G_s ” and the aforementioned properties of the glass. Figure 1-b illustrates a schematic of the radiation heat transfer through the two glass layers. Thus, according to figure 1-b, the transmitted radiation to the tubes “ $G_{s,tube}$ ” can be obtained using the following formula.

$$G_{s,tube} = (1 + \sum_{i=1}^{\infty} \rho^{2i}) \cdot \tau^2 \cdot G_s \quad (2)$$

On the other hand, the rate of heat transfer (\dot{Q}) can also be calculated as follows.

$$\dot{Q} = (\alpha_i \cdot G_{s,tube} - \varepsilon_i \cdot \sigma \cdot T_s^4) \cdot f \cdot A_i \quad (3)$$

where “ α_i ” and “ ε_i ” are the absorptivity emissivity of the black tubes, they are equal to 1. “ σ ” is the Stefan Boltzmann constant, it is equal to $5.67 \cdot 10^{-8} \text{ W} \cdot \text{m}^{-2} \cdot \text{K}^{-4}$. “ T_s ” is the average air tubes outside surface temperature. “ A_i ” is the lateral outside area of the tubes subjected to solar radiation. “ f ” is a surface fraction that varies between 0 and 1 since only a part of the tubes lateral area is subjected to the solar radiation.

Another equation of the rate of heat gain (\dot{Q}) is given as follows.

$$\dot{Q} = \frac{\Delta T_2}{R_t} \quad (4)$$

“ ΔT_2 ” is obtained using equation (5).

$$\Delta T_2 = T_s - T_a \quad (5)$$

Where “ T_a ” is the air temperature within the tubes. It is given by the following equation.

$$T_a = \frac{T_o + T_i}{2} \quad (6)$$

Where “ T_i ” is the air temperature at the inlet of the solar air heater) and “ T_o ” is the temperature of air leaving the solar air heater.

The total thermal resistance “ R_t ” is determined based on figure 1-c and using equation (7).

$$R_t = R_{conv,a} + R_{cond,t} \quad (7)$$

“ $R_{conv,a}$ ” is calculated using equation (8).

$$R_{conv,a} = \frac{1}{h \cdot (\pi \cdot d_i \cdot L)} \quad (8)$$

Where " d_i " is the inner diameter of the tubes and the convective heat transfer coefficient " h " is calculated using equations (9)-(11).

$$Re = \frac{\rho \cdot v \cdot d_i}{\mu} \quad (9)$$

$$Nu = 0.023 \cdot Re^{0.8} \cdot Pr^n \text{ for turbulent flow and } Nu = 3.66 \text{ for laminar flow} \quad (10)$$

Where " Re " is the Reynolds number of air, " v " is the speed of air within the tubes, " μ " is the dynamic viscosity of air determined at T_a , " Nu " is Nusselt number of air, " Pr " is the Prandtl number of air calculated at T_a and $n = 0.4$ for heating fluid case.

$$h = \frac{Nu \cdot k_a}{d_i} \quad (11)$$

Where " k_a " is the thermal conductivity of air calculated at T_a .

The conductive resistance of the tube " $R_{cond,t}$ " is calculated from equation (12).

$$R_{cond,t} = \frac{\ln(d_o / d_i)}{2 \pi k_t L} \quad (12)$$

Where " k_t " is the thermal conductivity of the tubes.

4. In-house code

In order to simulate numerically the solar air heater, an in-house code is developed in Excel software. This code is based on an iterative method solving the equations presented in the previous section in order to calculate the main outputs after initializing a set of inputs. The main outputs are: the tubes surface temperatures and the supply air temperature or the tubes length in addition to the efficiency of the solar air heater. The main input parameters that are considered are: the air inlet temperature, the properties of the tubes (inner diameter, outer diameter, absorptivity, emissivity, and conductivity), the solar irradiance, the surface fraction, the properties of the glass (absorptivity, reflectivity and transmissivity), the properties of air (conductivity, specific heat, density, and dynamic viscosity), the tubes length or the air supply temperature.

The calculation procedure consists of an initialization step and a calculation step. The first step consists of reading the main inputs while the second one consists of calculating the other parameters or the main outputs. Then, an iterative procedure is carried out to solve the system of equations. Figure 2 shows the flow diagram of the code.

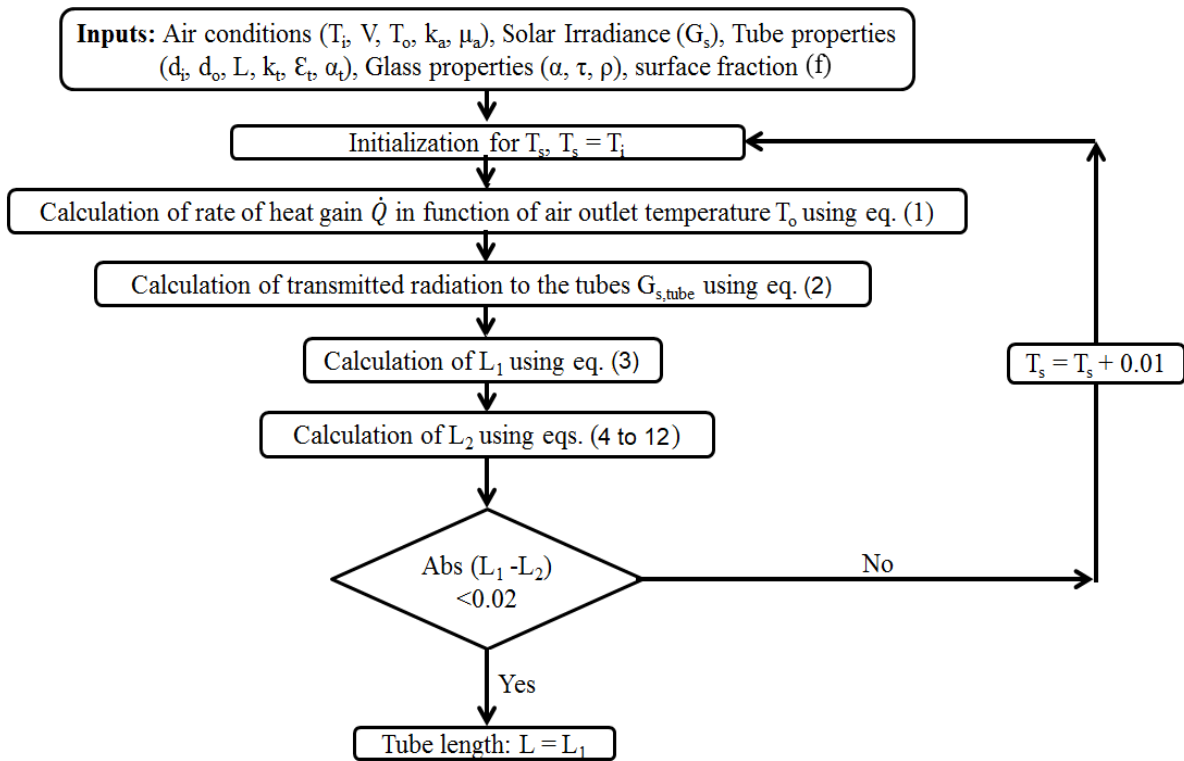


Fig. 2. Flow chart of the code

5. Experimental validation

An experimental study has been performed in order to validate the theoretical model presented in the previous section. For that purpose, a solar air heater that is composed of tubes that have characteristics presented in table 1 has been used. This solar air heater is similar to the one presented schematically in figure 1.

Table 1. Characteristics of solar air heater prototype

Tube material	Iron
Colour	Black
Length (m)	7.3
Inner Diameter (m)	0.032
Outer diameter (m)	0.035
Shape	hairpin

The solar air heater system is made of a box holding the black tubes. This box is covered by double glass cover. A valve is placed at the outlet of the tubes to control the flow rate and a fan is used to circulate the air inside the tubes. Also, the whole system is inclined by 35° with respect to the horizontal. Figure 3-a shows the iron tubes of the solar air heater system and figure 3-b shows the whole prototype.

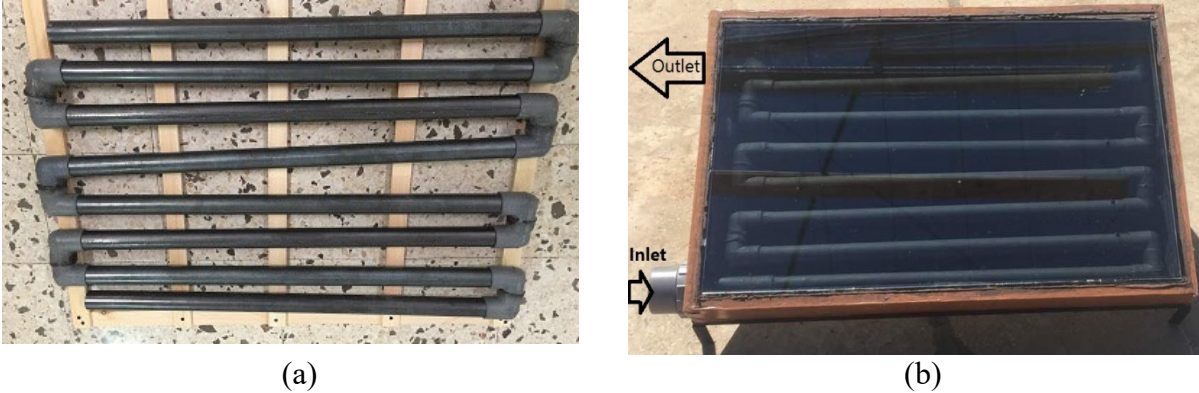


Fig. 3. (a) the iron tubes of the solar air heater system and (b) the solar air heater prototype

5.1. Procedure for tests

In order to get the required results, two thermocouples with $\pm 1\%$ incertitude are used to measure the temperatures of the air at the inlet and exit of the SAH, an anemometer with an uncertainty of $\pm 1\%$ is placed at the tubes outlet and is used to measure the air speed within the tubes which is regulated by a gate valve and a pyrometer is used to measure the solar irradiance. Different tests have been performed for different air speeds, with an ambient air of 26°C and solar irradiance of 400 W/m^2 .

Since the comparison between experimental and numerical air outlet temperatures is based on the air flow inside the pipes, uncertainty analysis is considered on the air speed inside the pipes whose variation is repeated twice under the same operating conditions and then for four different operating conditions. This lead to a total of 8 tests. A maximum difference of 0.4 m/s was obtained leading to 0.5% relative difference. Moreover, the error of positioning the anemometer in the pipe is 0.1 m/s with a minimum speed of 1.5 m/s . This leads to a maximum relative error due to this positioning method of 6.6% . This 0.5% repeatability and 6.6% precision error gives an uncertainty of 6.61% or 93.39% confidence in flow or speed measurements. The same method is applied to the temperatures measurements and a confidence of 95.4% is obtained.

5.2. Results and comparison

Table 2 and figure 4 present a comparison between theoretical and experimental results based on the air outlet temperature for different air speeds and then different mass flow rates. The surface fraction “ F ” is taken equal to 0.5 in this case which means that only the upper surface of the lateral area of the tubes is considered to be subjected to the solar radiation. Moreover, the maximum air speed is limited to 6 m/s due to high noise pollution that may result from high air speeds in pipes.

Table 2. Comparison between the model and experiments

T inlet (°C)	ρ (kg/m ³)	V _a (m/s)	\dot{m} (kg/s)	T outlet (°C)		
				Numerical	Experimental	Error (%)
26	1.17	1.50	0.0014	107	96	10.28
26	1.17	2.50	0.0023	74.8	65.5	12.43
26	1.17	4.00	0.0037	56.6	59.2	-4.59
26	1.17	6.00	0.0055	46.4	53	-14.22

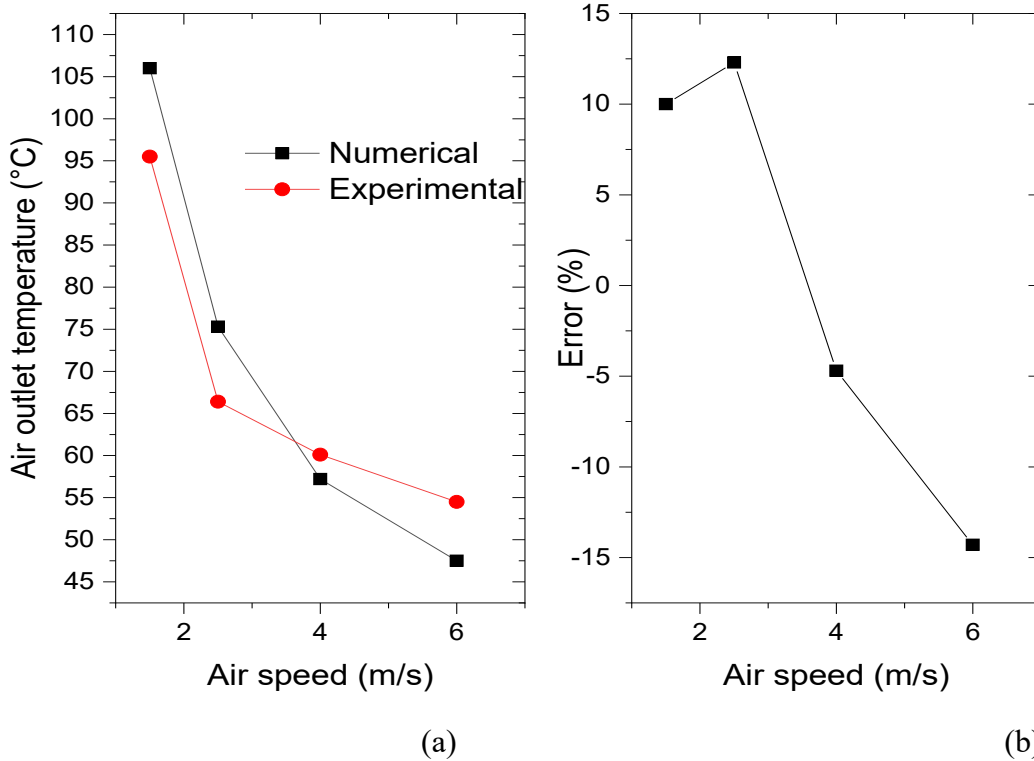


Fig 4. (a) air outlet temperature comparison between model and experiment and (b) air outlet temperature error between model and experiment

The main conclusions from table 2 and figure 4 are presented as follows:

- When the air speed increases within the tubes, the air outlet temperature decreases for both, the model and the experiment. This increasing in air speed leads to an increase in the mass flow rate. For a same heat gain, increasing the mass flow rate causes a decreasing in the outlet temperature.
- The absolute value of the error on the air outlet temperature between the model and the experiment is always below 15%.
- For an air speed of 2.5 m/s, the air outlet temperatures of the model and the experiment are 74.8°C and 65.5°C respectively. The error on the air outlet temperature is then around 12.4%.
- For an air speed of 4 m/s, the air outlet temperatures of the model and the experiment are 56.6°C and 59.2°C respectively. The error on the air outlet temperature is then around 4.6%.

The results presented in Fig. 4 permit to conclude that the developed code is strengthened and accurate enough to be used as a simulator for the suggested solar air heater especially that the error is always lower than 14% for an air speed varying between 1 and 6 m/s. Furthermore, the results reveal that the temperature of the supply air is in the temperature range [50-80°C] suitable for drying fruits and this solar air heater could be able to supply hot air for a fruit dryer.

6. Case study on fruit dryer

6.1. Economic analysis

As proved previously, the solar air heater was able to heat up an air flow to a temperature range that is suitable for food drying and it then could replace an electric fruit dryer as shown in figure 5. For that purpose, a 1 kW electrical food dryer, 35 °C to 70 °C temperature range suitable for drying food and fruits, maximum capacity of 18 kg/batch and maximum drying time of 15 hours is taken under study for the case in Lebanon. The study aims to quantify the amounts of electrical energy and cost saved when drying fruits like cherry using a dryer supplied by a solar air heater instead of an electric dryer.

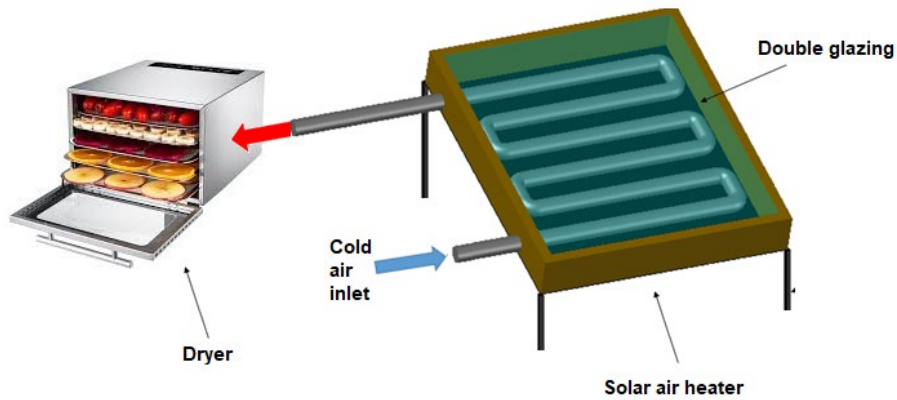


Fig. 5. Solar air heater coupled to a fruit dryer

The yearly energy saved or reduced by using a dryer supplied by a solar air heater instead of an electric dryer is determined using equations (13) and (14).

$$E_{reduced/month} = P_{input} \cdot t_d \cdot N \cdot P \quad (13)$$

where “ $E_{reduced/month}$ ” is the energy reduced per month (kW.hr/month), “ P_{input} ” is the input power (kW), “ t_d ” is the drying time (15 hr/batch), “ N ” is the number of batches per month. Table 3 presents the number of batches and the corresponding mass of dried cherry. P is the portion of drying time that is recovered (from 10 to 100%).

Table 3. Number of batches and mass of dried food per month.

N (batch/month)	4	8	12	16
Mass of dried cherry (kg/month)	72	144	216	288

$$E_{reduced/year} = E_{reduced/month} \cdot 12 \quad (14)$$

where “ $E_{reduced/year}$ ” is the energy reduced per year (Kw.hr/year).

Figure 6-a shows the variation of $E_{reduced/year}$ as function of P.

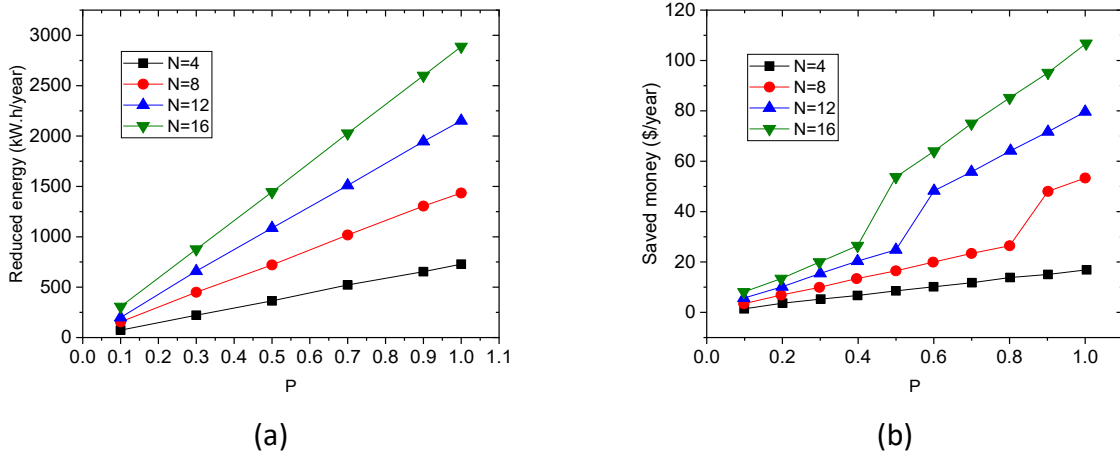


Fig. 6. (a) Variation of $E_{reduced/year}$ as function of P, (b) Variation of saved money in terms of P

Figure 6-a shows that the energy saved is directly related to P. This amount rises from 72 to 720, 144 to 1440, 216 to 2160 and from 288 kWh/year to 2880 kWh/year when P increases from 10 to 100% for N equal 4, 8, 12 and 16 respectively. Besides, it is revealed obtained that this amount increases when the number of batches increases. As illustration, it is equal to 60 kWh at N = 8 and increases to 90 kWh at N = 12 for P = 0.5.

After calculating the amount of energy saved, the amount of money saved can be calculated by using equations (15) and (16).

$$SM / Month = E_{reduced/month} \cdot P_{1kw.hr} \quad (15)$$

where “ $SM / Month$ ” is the monthly saved money (\$/month) and “ P_{1Kwhr} ” is the price of producing an electrical energy of 1 kWh. For Lebanon case, the price of first 99 kWh is 0.023 \$; however, above 100 kWh the price becomes 0.037\$.

$$SM / Year = SM / Month \cdot 12 \quad (16)$$

where “ $SM / Year$ ” is the annual amount of money saved (\$/year).

Figure 6-b shows the variation of $SM / Year$ in terms of P . When P increases, $SM / Year$ increases. As illustration, when P increases from 0 to 1, the amount of money saved increases from 1.65 to 16.56, 3.31 to 53.28, 4.96 to 79.92 and from 6.62 to 106.56 \$/year for N equal 4, 8, 12 and 16 respectively. Besides, it is also revealed obtained that this amount increases when the number of batches increases. As illustration, it is equal to 16.56 \$/year at $N = 8$ and increases to 24.84 \$/year at $N = 12$ for $P = 0.5$.

6.2. Environmental analysis

The dryer supplied by a solar air heater permit to decrease the emissions to the environment. To evaluate this decreasing, the same electric dryer (used in the previous section) is taken under study. Equation (17) presents the amount of reduced CO_2 emission.

$$M_{reduced,CO_2} = E_{reduced/year} \cdot M_{CO_2/1kWhr} \quad (17)$$

where “ $M_{reduced,CO_2}$ ” is the mass of reduced CO_2 emission (kg), “ $M_{CO_2/1kWhr}$ ” is the mass of CO_2 generated from 1 kWh electricity (0.71 kg CO_2 /1 kWh for the case of Lebanon).

Figure 7 shows the annual variation of the mass of emission in terms of P .

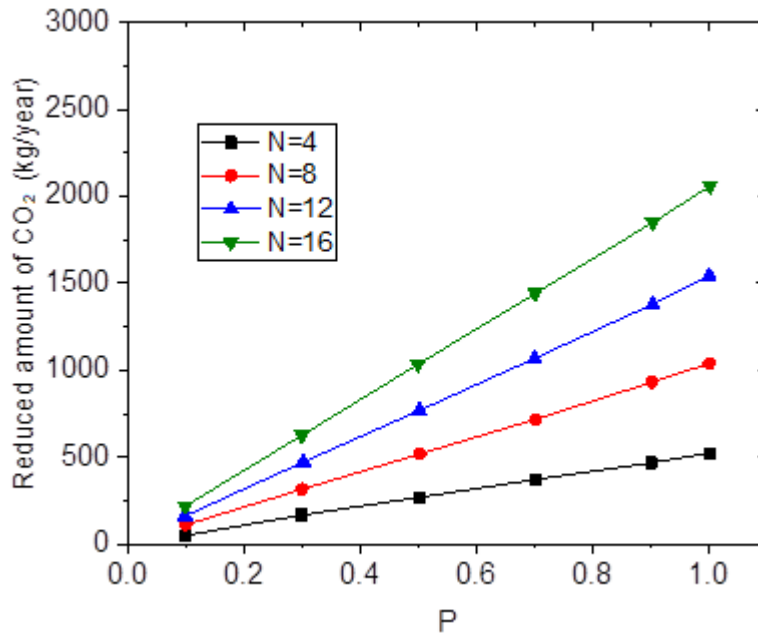


Fig. 7. Mass of reduced CO_2 emission variation in terms of P .

As shown in figure 7, the amount of reduced CO₂ emission is directly related to P. This amount rises from 51.12 to 511.2, 102.24 to 1022.4, 153.36 to 1533.6 and 204.48 to 2044.8 kg when P increases from 10 to 100% for N equal 4, 8, 12 and 16 respectively.

Besides, it is also revealed obtained that this amount increases when the number of batches increases. As illustration, it is equal to 511.2 kg at N = 8 and increases to 766.8 kg at N = 12 for P = 0.5.

7. Conclusions

A solar air heater is proposed as a solution to reduce energy consumption and environmental emission. The system allows direct heating of air using black tube covered by double glass cover. A fan is utilized to provide the air flow which is in turn controlled by an air valve. An in-house code is performed to simulate the solar air heater in order to size the system as well as to carry-out parametric studies. An experimental study is performed and is used to validate the code. Numerical results compare well with their experimental counterparts where the error varies between 4 % and 15 % depending on the configuration. Furthermore, a fruit dryer is considered as case study in order to evaluate comprehensively the proposed concept economically and environmentally. It has been shown that using the proposed solar air heater to supply a fruit dryer permits to save up to \$106 per year and to reduce Carbon dioxide emission by 2044.8 kg.

References

- [1] M. Khaled, F. Harambat, H. El Hage, and H. Peerhossaini, Spatial optimization of underhood cooling module – towards an innovative control approach, *Applied Energy*, 88 (2011) 3841-3849.
- [2] M. Khaled, F. Harambat, and H. Peerhossaini, Towards the control of car underhood thermal conditions, *Applied Thermal Engineering*, 31 (2011) 902-910.
- [3] M. Khaled, F. Harambat, and H. Peerhossaini, Temperature and Heat Flux Behavior of Complex Flows in Car Underhood Compartment, *Heat Transfer Engineering*, 31-13 (2010) 1-11.
- [4] J. Wang, J. Liu, C. Li, Y. Zhou and J. Wu, Optimal scheduling of gas and electricity consumption in a smart home with a hybrid gas boiler and electric heating system. *Energy*, 204 (2020), 117951.
- [5] S. Adegbite, W. Asiru, M. Sartas, T. Tran, A. Taborda, A. Chapuis, M. Ojide and A. Abass, Development of a pilot scale energy efficient flash dryer for cassava flour. *Resources, Environment and Sustainability*, 13 (2023), 100117.
- [6] D. Ivanova, K. Enimanev and K. Andonov, Energy and economic effectiveness of a fruit and vegetable dryer. *Energy Conversion and Management*, 44 (2003), Issue 5, 763-769.

- [7] J. Li, X. Yan, M. Zhang, Y. Xu, E. Meng and Q. Li, Simulation and analysis of a new cabinet heat pump clothes dryer. *International Communications in Heat and Mass Transfer*, 143 (2023), 106688.
- [8] Z. Zhi, Z. Ming, Y. Bo, G. Zun, W. Zhaoyuan and L. Gengyin, Multipath retrofit planning approach for coal-fired power plants in low-carbon power system transitions: Shanxi Province case in China. *Energy*, 275 (2023), 127502.
- [9] K. Faraj, M. Khaled, J. Faraj, F. Hachem, K. Chahine, and C. Castelain, Energetic and economic analyses of integrating enhanced macro-encapsulated PCM's with active underfloor hydronic heating system, *Energy Reports*, 8 (2022) 848-862.
- [10] Z. Wehbi, R. Taher, J. Faraj, M. Ramadan, C. Castelain, and M. Khaled, A Short Review of Recent Studies on Wastewater Heat Recovery Systems: Types and Applications, *Energy Reports*, 8 (2022) 896-907.
- [11] K. Faraj, M. Khaled, J. Faraj, F. Hachem, K. Chahine, and C. Castelain, Short recent summary review on evolving phase change material encapsulation techniques for building applications, *Energy Reports*, 8 (2022) 1245-1260.
- [12] O. Farhat, M. Khaled, J. Faraj, F. Hachem, R. Taher, and C. Castelain, A short recent review on Hybrid Energy Systems: Critical Analysis and Recommendations, *Energy Reports*, 8 (2022) 792-802.
- [13] Z. Wehbi, R. Taher, J. Faraj, C. Castelain and M. Khaled, Hybrid Thermoelectric Generators-Renewable Energy Systems: A Review on Recent Developments, *Energy Reports*, 8 (2022) 1361-1370.
- [14] F. Afshari, E. Mandev, B. Muratçobanoğlu, A. Yetim, M. Ceviz. Experimental and numerical study on a novel fanless air-to-air solar thermoelectric refrigerator equipped with boosted heat exchanger, *Renewable Energy*, 207 (2023), 253-265.
- [15] F. Afshari, B. Muratçobanoğlu, E. Mandev, M. Ceviz, Z. Mirzaee. Effects of double glazing, black wall, black carpeted floor and insulation on thermal performance of solar-glazed balconies, *Energy and Buildings*, 285 (2023), 112919.
- [16] E. Douvi, C. Pagkalos, G. Dogkas, M. K. Koukou, V. N. Stathopoulos, Y. Caouris, and M. Gr. Vrachopoulos, Phase change materials in solar domestic hot water systems: A review, *International Journal of Thermofluids*, 10 (2021) 100075.
- [17] E. Matjanov, Z. Akhrorkhujajeva, Solar repowering existing steam cycle power plants, *International Journal of Thermofluids*, 17 (2023) 100285.
- [18] E. Elshazly, A. A. Abdel-Rehim, and I. El-Mahallawi, Thermal performance enhancement of evacuated tube solar collector using MWCNT, Al₂O₃, and hybrid MWCNT/ Al₂O₃ nanofluids, *International Journal of Thermofluids*, 17 (2023) 100260.

- [19] A. M.A. Alshibil, I. Farkas, and P. Víg, Multi-aspect approach of electrical and thermal performance evaluation for hybrid photovoltaic/thermal solar collector using TRNSYS tool, *International Journal of Thermofluids*, 16 (2022) 100222.
- [20] A.D. Dhass, D. Patel, and B. Patel, Estimation of power losses in single-junction gallium-arsenide solar photovoltaic cells, *International Journal of Thermofluids*, 17 (2023) 100303.
- [21] R. Karwa, Thermo-hydraulic performance of solar air heater with finned absorber plate forming multiple rectangular air flow passages in parallel under laminar flow conditions, *Applied Thermal Engineering*, 221 (2023) 119673.
- [22] H. Farzan and E. H. Zaim, Study on thermal performance of a new combined perforated Metallic/Asphalt solar air heater for heating Applications: An experimental study, *Solar Energy*, 249 (2023) 485-494.
- [23] H. K. Ghritlahre, M. Verma, J. S. Parihar, D. S. Momdloe, and S. Agrawal, A detailed review of various types of solar air heaters performance, *Solar energy*, 237 (2022) 173-195.
- [24] A. Kocer, I. Atmaca and C. Ertekin, A comparison of flat plate and evacuated tube solar collectors with F-Chart method, *Journal of Thermal Science and Technology*, 35 (2015), 1, 77-86.
- [25] S. Kalogirou, Solar thermal collectors and applications. *Progress in Energy and Combustion Science*, 30 (2004), 231–295.
- [26] A. A. Hegazy, Optimum channel geometry for solar air heaters of conventional design and constant flow operation, *Energy Conversion and Management*, 40 (1999) 757-774.
- [27] A. Kumar, Akshayveer, A. P. Singh, and O.P. Singh, Investigations for efficient design of a new counter flow double-pass curved solar air heater, *Renewable Energy*, 185 (2022) 759-770.
- [28] S. Chand, P. Chand, and H. K. Ghritlahre, Thermal performance enhancement of solar air heater using louvered fins collector, *Solar Energy*, 239 (2022) 10-24.
- [29] C. Arkar, T. Šuklje, B. Vidrih, and S. Medved. Performance analysis of a solar air heating system with latent heat storage in a lightweight building, *Applied Thermal Engineering*, 95 (2016) 281-287.
- [30] H. El Hage, A. Herez, M. Ramadan, H. Bazzi, and M. Khaled, An investigation on solar drying: A review with economic and environmental assessment, *Energy*, 157 (2018) 815-829.
- [31] R. K. Srivastava and A. K. Rai. A review on solar air heater technology. *International Journal of Mechanical Engineering and Technology*, 8 (2017) 1122–1131.

[32] R. Kumar and S. K. Verma, Performance estimation of Triangular Solar air heater roughened absorber surface: An experimental and simulation modeling, *Sustainable Energy Technologies and Assessments*, 52 (2022) 102208.

[33] B. Lamrani, F. Kuznik, A. Ajbar, and M. Boumazac, Energy analysis and economic feasibility of wood dryers integrated with heat recovery unit and solar air heaters in cold and hot climates, *Energy*, 228 (2021) 120598.